Effect of local atomic and electronic structures on thermoelectric properties of chemically substituted CoSi

2014 EPL 106 37007

(http://iopscience.iop.org/0295-5075/106/3/37007)

A Letters Journal Exploring the Frontiers of Physics

May 2014

EPL, **106** (2014) 37007 www.epljournal.org
doi: 10.1209/0295-5075/106/37007

Effect of local atomic and electronic structures on thermoelectric properties of chemically substituted CoSi

C. C. Hsu[1], C. W. Pao[1], J. L. Chen[1], C. L. Chen[2(a)], C. L. Dong[1(b)], Y. S. Liu[3], J. F. Lee[1], T. S. Chan[1], C. L. Chang[3], Y. K. Kuo[4] and C. S. Lue[5]

[1] *National Synchrotron Radiation Research Center - Hsinchu 30076, Taiwan*
[2] *Institute of Physics, Academia Sinica - Taipei 11529, Taiwan*
[3] *Department of Physics, Tamkang University - Taipei 25137, Taiwan*
[4] *Department of Physics, National Dong Hwa University - Hualien 97404, Taiwan*
[5] *Department of Physics, National Cheng Kung University - Tainan 70101, Taiwan*

received 12 February 2014; accepted in final form 17 April 2014
published online 9 May 2014

PACS 78.70.Dm – X-ray absorption spectra
PACS 61.05.cj – X-ray absorption spectroscopy: EXAFS, NEXAFS, XANES, etc.
PACS 73.50.Lw – Thermoelectric effects

Abstract – We report the effects of Ge partial substitution for Si on local atomic and electronic structures of thermoelectric materials in binary compound cobalt monosilicides ($CoSi_{1-x}Ge_x$: $0 \leq x \leq 0.15$). Correlations between local atomic/electronic structure and thermoelectric properties are investigated by means of X-ray absorption spectroscopy. The spectroscopic results indicate that as Ge is partially substituted onto Si sites at $x \leq 0.05$, Co in $CoSi_{1-x}Ge_x$ gains a certain amount of charge in its 3*d* orbitals. Contrarily, upon further replacing Si with Ge at $x \geq 0.05$, the Co 3*d* orbitals start to lose some of their charge. Notably, thermopower is strongly correlated with charge redistribution in the Co 3*d* orbital, and the observed charge transfer between Ge and Co is responsible for the variation of Co 3*d* occupancy number. In addition to Seebeck coefficient, which can be modified by tailoring the Co 3*d* states, local lattice disorder may also be beneficial in enhancing the thermoelectric properties. Extended X-ray absorption fine structure spectrum results further demonstrate that the lattice phonons can be enhanced by Ge doping, which results in the formation of the disordered Co-Co pair. Improvements in the thermoelectric properties are interpreted based on the variation of local atomic and electronic structure induced by lattice distortion through chemical substitution.

Introduction. – At present, energy crisis and extreme climate are two of the most pressing global issues believed to be related to the rise in carbon dioxide emission. Sunlight is a clean, renewable, and abundant energy resource that can be converted into electricity through a solar cell, wherein solar energy excites the cell's electrons. Utilizing solar energy is one of the best ways to generate green energy. To date, the highest performance efficiency attained by commercial solar cells varies between 10% to 20%, with a substantial portion of energy lost due to heat loss to the environment. The problem is how to fully utilize the waste heat and make the use of solar energy more efficient. Solar cells only absorb a certain wavelength of sunlight, but heat has no such restrictions. Thus, thermoelectric materials that can convert temperature gradient into thermal induced current may be promising candidates for energy applications [1].

Transition metal silicides with semi-metallic or semiconducting properties have drawn much attention due to their applications in thermoelectric materials [2–5]. Silicides exhibit great stability and chemical resistance to oxidation or acidification due to their strong covalent bonding, making them more suitable for a practical range of applications, including those performed in high temperature. Among silicides, cobalt monosilicide CoSi is regarded as a high-potential candidate for thermoelectric applications [6–8]. CoSi is a semi-metal, and band structure calculations have shown the presence of a narrow gap, also known as pseudogap, at the Fermi level in its density of states (DOS).

(a) E-mail: clchen@phys.sinica.edu.tw
(b) E-mail: dong.cl@nsrrc.org.tw

Materials with pseudogaps have been suggested to have potential as good thermoelectric materials [9].

In general, the efficiency of a thermoelectric material is evaluated by the dimensionless figure of merit ZT, calculated as $ZT = S^2\sigma T/\kappa$, where S is the thermopower (Seebeck coefficient), σ is the electrical conductivity, and κ is the thermal conductivity composed of the lattice contribution ($\kappa_{\rm L}$) and electronic contribution ($\kappa_{\rm e}$). A higher ZT value denotes better energy conversion efficiency of a thermoelectric material. Consequently, the criteria of a thermoelectric material are defined as follows: higher Seebeck coefficient; lower electrical resistivity; and lower thermal conductivity. Conceptually, by properly adjusting the parameters S, σ, and κ, the figure of merit ZT can be enhanced facilely. Unfortunately, according to the Weideman-Franz law, an increase of the electrical conductivity (σ) results in a corresponding increase in thermal conductivity ($\kappa_{\rm e}$), which is an obstacle in achieving a high ZT. The dilemma of allowing electrical transport while simultaneously blocking thermal transport can be addressed by reducing the lattice phonons [6,10]. Current strategy optimizes these two conflicting parameters, which are usually targeted as the charge carrier increases, by doping and enhancement of phonon scattering by introducing crystallographic disorder. Numerous studies have been conducted based on adjusted parameters among S, σ, and κ to discover thermoelectric materials with high performance [8]. Notably, all these effects are closely related to their atomic and electronic structure around the Fermi level, making these suitable for investigation through X-ray spectroscopy. To our knowledge, the thermoelectric properties of such materials have been rarely elucidated in terms of atomic/electronic structures. Therefore, to improve the thermoelectric efficiency of CoSi, tuning its physical properties was accomplished by Ge substitution on the Si sites. In this study, we investigated the effects of chemical substitution on the thermoelectric properties through X-ray absorption spectroscopy (XAS).

Experimental. – $CoSi_{1-x}Ge_x$ alloys with $0 \leq x \leq 0.15$ were prepared by arc melting [8]. The mixture of high-purity elements was placed in a water-cooled copper crucible under an argon atmosphere. These alloys were then arced several times to attain better sample homogeneity. Sample quality and structural analysis were characterized by powder X-ray diffraction with Cu $K\alpha$ radiation as the cubic B20 structure. XAS measurements were performed at the National Synchrotron Radiation Resyearch Center (NSRRC), Taiwan. XAS at Co, Ge K-, and Co L-edges were performed at the wiggler beamline 17C using the transmission mode and the HSGM beamline 20A using total electron yield mode at room temperature. The electronic and atomic structures revealed by XAS are compared with thermoelectric properties, such as Seebeck coefficient and thermal conductivity measured at room temperature [8]. The monochromator Si (111) crystals were used in the wiggler beamline 17C

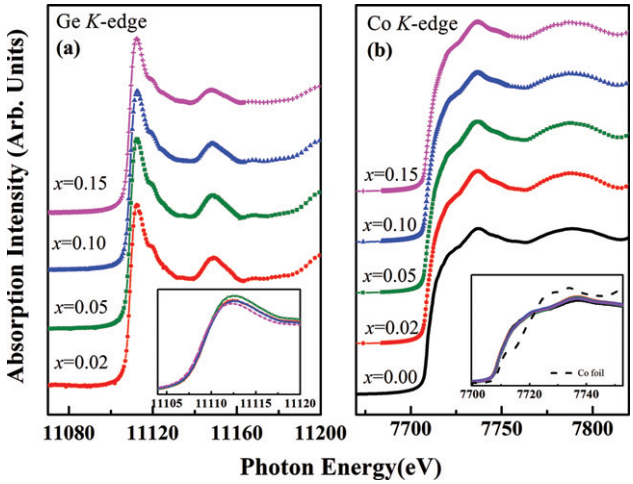

Fig. 1: (Colour on-line) XAS spectra of (a) Ge K-edge and (b) Co K-edge of $CoSi_{1-x}Ge_x$ with x = 0–0.15. Insets show the magnified area of the main peak region.

with energy resolution set to 0.5 eV to 0.7 eV at Co (Ge) K-edge. The energy resolution at HSGM beamline 20A was set to 0.2 eV. Extended X-ray absorption fine structure (EXAFS) oscillations were isolated by removal of the subsequent pre-edge background by using Athena software. Resulting EXAFS curves in the wave-vector space $\chi(k)$ were weighted by k^3, Fourier transformed with Athena code, and fitted using the Artemis program of the IFEFFIT [11]. Structural parameters were thus estimated, including coordination number, bond length (R) and Debye-Waller factor (DWF) (σ^2).

Results and discussion. – Materials with narrow gaps and large DOS at the Fermi level have been suggested to possess good potential as thermoelectric materials [1,12]. Thus, the electronic structures around the Fermi level are significant and can be determined by X-ray spectroscopy. Figures 1(a) and (b) present the Co and Ge K-edge spectra, respectively. The insets show the overlaid spectra so the change in peak intensity can be observed. Ge K-edge originates from the excitation of the 1s core electron to the unoccupied 4p orbitals. Evidently, all spectra of Ge K-edge are similar, implying that the overall crystal structure remains unchanged upon Ge doping. However, the inset of fig. 1(a) shows that the peak intensity differed with the substitution of Ge for Si in $CoSi_{1-x}Ge_x$ (x = 0.02 to 0.15), suggesting that electronic structure may vary among the samples. The peak intensity is apparently increased from x = 0.02 to 0.05 and then decreased beyond x = 0.05, suggesting the occurrence of more Ge 4p unoccupied states at x = 0.05, which declines beyond this value (x = 0.05). The change in 4p states of dopant Ge implies that the 4p orbital loses charge until x = 0.05, but gains charge when $x > 0.05$. This result indicates a corresponding charge redistribution with the increase in dopant concentration. Therefore, the

electron DOS becomes critical from the perspective of the Co site. Figure 1(b) displays the Co K-edge spectrum ascribed to the electronic transition mainly from the Co 1s to 4p states. The overall spectral profiles resemble each other, again suggesting the unchanged crystal structure upon Ge doping, which is in agreement with the result from Ge K-edge. The inset of fig. 1(b) further compares the peak intensities of CoSi with different Ge contents, showing that the peak intensities of $CoSi_{1-x}Ge_x$ are not influenced by Ge doping. The insignificant change in Co K-edge indicates that apart from the electronic DOS at the Co 4p orbital, the lattice structure is also quite similar at the Co site. No significant variation of lattice structure is observed in $CoSi_{1-x}Ge_x$, which is consistent with the XRD results [8].

However, while the outermost electron shell in Ge is the 4p orbital, the 3d orbital is the outermost shell of electron in Co. Instead of the 4p orbital that is probed by Co K-edge XAS, Co 3d states can be directly probed by the Co L-edge owing to the transition from $2p^6d^7$ to $2p^5d^8$ final states. The thermoelectric properties are strongly correlated with the DOS of d orbital [12–16]. Thus, the Co L-edge may provide more detailed information on the electronic structure than the K-edge. Figure 2(a) displays the Co L-edge spectra. In the Co L-edge XAS in fig. 2(a), the spin-orbital coupling splits the Co 2p core hole into the $2p_{3/2}$ and $2p_{1/2}$ levels, yielding the Co L_3- and Co L_2-edges that originate from the $V\,2p_{3/2} \rightarrow V\,3d$ and $V\,2p_{1/2} \rightarrow V\,3d$ transitions, respectively. Normally, the L_2-edge is the replica of L_3-edge: in this case, the enlargement of the L_3 absorption edge is given in fig. 2(b). The absorption peak of Co L_3-edge at $x = 0.05$ presents the lowest intensity. The integrated intensity across the Co L_3 absorption edge after removing the transition to the continuum states (marked by the dashed lines in the bottom of fig. 2(a)) is proportional to the density of unoccupied Co 3d states. These integrated values are presented in fig. 2(c).

Notably, the unoccupied Co 3d states do not vary systematically with x in these $CoSi_{0.95}Ge_{0.05}$ samples. Calculated DOS studies have indicated that the Co 3d states are mainly confined near the Fermi level in $CoSi_{1-x}Ge_x$ alloys [15]. Seebeck coefficient is often discussed using the Mott formula, which suggests that any change in the Seebeck coefficient is a direct effect of the modifications in the DOS near the Fermi level [8,12]. The Seebeck coefficient measurement is a sensitive energy probe relative to the Fermi level, and these results could reveal information about the changes in band/electronic structure. Therefore, in addition to the unoccupied Co 3d states plotted in fig. 2(c), the relation to S is also included for comparison. Interestingly, the measured S does not vary in relation to x in the $CoSi_{1-x}Ge_x$ alloys, but the change in S correlates well with the unoccupied Co 3d states, indicating that the observed composition dependence in S is likely attributed to the changes in the density of Co 3d states [15].

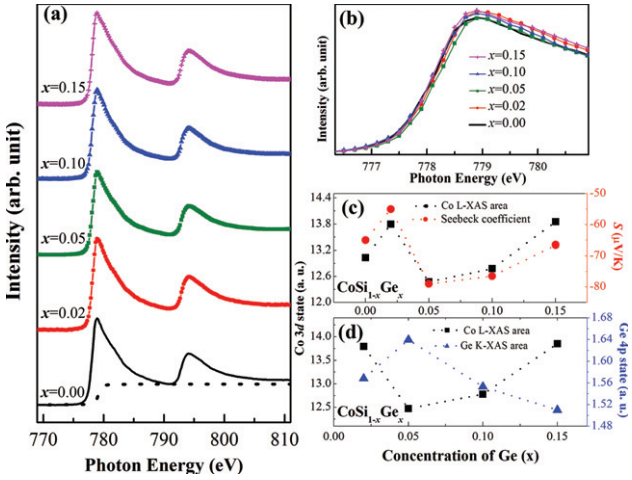

Fig. 2: (Colour on-line) (a) XAS spectra of Co $L_{2,3}$-edges of $CoSi_{1-x}Ge_x$ with x = 0–0.15. (b) Overlaid spectra of L_3-edge area. (c) Relation of Co 3d states and thermopower S. (d) Comparison of peak intensities from Co L-edge and Ge K-edge.

To gain insight into the origin of the change in Co 3d density of states modified by Ge dopant, the electronic structure around host Co and dopant Ge sites are compared in fig. 2(d). As previously stated, the change in the 4p states of dopant Ge implies that the 4p orbital loses charge until $x = 0.05$ and gains charge when $x > 0.05$, indicating the occurrence of charge redistribution in $CoSi_{1-x}Ge_x$ with increased dopant concentration. To qualitatively estimate the change of unoccupied 4p states of the dopant, the same procedure is exploited (method used in Co L_3-edge). The peak area across the Ge K-edge is integrated after discounting the background intensity generated from the transition to continuum states. These values are expected to be proportional to the density of unoccupied Ge 4p states, as presented in fig. 2(d). Notably, the absorption peak of Co L-edge at $x = 0.05$ presents the lowest intensity, whereas the Ge K-edge at $x = 0.05$ presents the highest intensity. Moreover, opposite trends of the peak areas estimated from Co L- and Ge K-edges are observed. As reported earlier in CoSi band structure calculations [14–16], CoSi is characterized as a semi-metal and shows a slight overlap between electron and hole pockets, yielding a small DOS around the Fermi level which facilitates the charge transfer between Ge (4p) and Co (3d) hybridized states. These results show that the occupation of the Co 3d states decreases (increases) with corresponding increased (decreased) Ge 4p occupation upon Ge doping. The experimental observation suggests the occurrence of charge transfer between Co and Ge.

Variation in DOS near the Fermi level, which is associated with pseudogap narrowing, is responsible for the observed composition dependence in the Seebeck coefficient of $CoSi_{1-x}Ge_x$ [8]. The band structure of $CoSi_{1-x}Ge_x$

exhibits a slight extension of the pseudogap, making a shift toward Fermi level in the increase of Ge substitution for Si [17]. The narrowing of the pseudogap may increase Ge 4*p*-Co 3*d* hybridization. By considering the electronegativity of Co (1.88), Si (1.9), and Ge (2.01), Ge has higher electronegativity than Co; thus, with a greater Ge amount in the system, the *p*-*d* hybridization of Co (3*d*) and Ge (4*p*) is enhanced, resulting in increased Ge charges acquired from Co.

The mobility of the charge carrier may correlate with the empty states in the conduction band, so the DOS at E_{F} may be associated with electrical resistivity. In reference to the electrical resistivity measurements, CoSi alloys exhibit semi-metallic behavior. Upon a slight degree of Ge substitution ($x < 0.02$) for Si, the electrical resistivity exhibits a significant decrease by about an order of magnitude [8]. With further Ge substitution, the electrical resistivity continuously decreases. The semi-metallic nature and the decrease in resistance have been associated with the low DOS at the Fermi level (E_{F}).

Substitution of Ge in $CoSi_{1-x}Ge_x$ alloys is expected to yield larger atomic radius than that of Si, which enables an extended *p* orbital to overlap with Co 3*d* and consequently narrow the band gap. This gap narrowing may lead to an increase in DOS at E_{F} for these Ge-substituted alloys, resulting in a reduction in electrical resistivity. However, the thermopower cannot be fully explained by the change of DOS at E_{F}, and the relation of S behavior and electronic structure around Co is only valid at x-values beyond 0.05. Consequently, another factor possibly dictates thermopower. The Seebeck coefficient is theoretically proportional to the slope of DOS around the Fermi level, and a slight shift in the position of Fermi level could cause a substantial change in Seebeck coefficient [12]. The measured Seebeck coefficient does not vary systematically with Ge content at room temperature, which is due to the fact that the Seebeck coefficient not only depends on the electronic DOS but on the relative position to the Fermi level. For high Ge doping level, the band structure exhibiting the pseudogap slightly extends to make a shift toward Fermi level with the increase of Ge substitution for Si [17]. Consequently, the different behaviors of relation between S and Co 3*d* states below and above $x = 0.05$ may originate from the different positions of E_{F}. More detailed calculation is required to clarify this argument.

The ability of a material to efficiently produce thermoelectric power is related to its dimensionless figure of merit, given by $ZT = S^2\sigma T/\kappa$. ZT value can be optimized by adjusting the parameters of S, σ, and κ. Normally, good electrical conductivity and poor thermal conductivity will yield a high ZT value. To enhance ZT, increasing the electrical conductivity is commonly achieved by doping. However, total thermal conductivity (κ) is a sum of electronic (κ_{e}) and lattice (κ_{L}) terms, which is written as $\kappa = \kappa_{\mathrm{L}}+\kappa_{\mathrm{e}}$. Therefore, increasing electrical conductivity (σ) will spontaneously increase the electric contribution (κ_{e}) of thermal

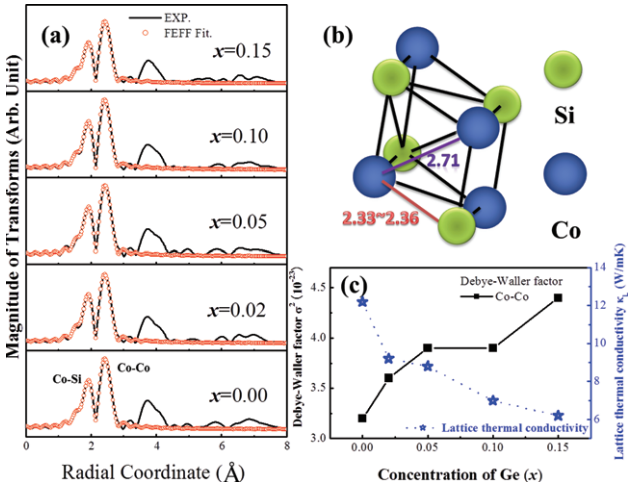

Fig. 3: (Colour on-line) (a) k^3-weighted Fourier-transformed EXAFS spectra Black solid lines represent experimental data and red open circles represent best-fitted spectra. (b) Local structure of CoSi. (c) Correlation of lattice thermal conductivity and Debye-Waller factor.

conductivity (κ) based on Wiedemann-Franz law, which is stated as $\kappa_{\mathrm{e}} = L_0T/\rho$, where ρ is the electric resistivity and the Lorentz number. Thus, this situation retards ZT enhancement. An increase in the electrical contribution of thermal conductivity inevitably results from increasing the electrical conductivity, so a current strategy is to reduce the lattice thermal conductivity by enhancing the phonon scattering by introducing crystallographic disorder [18]. The foregoing highlights the significance of lattice phonon in the study. The lattice phonon can be revealed by DWF (σ^2) from EXAFS.

Figure 3(a) presents the κ^3-weighted Fourier-transformed EXAFS spectra from $k = 3.2$ to 13.2 Å^{-1} (black solid lines) of the $CoSi_{1-x}Ge_x$ samples. The best fits (open red circles) to the spectra are also plotted in fig. 3(a). The results of the best fits for the shells are given in table 1. The R-factor is a measure of the misfit between theoretical and experimental Fourier transformed spectrum and can be used to evaluate the goodness of fit. The R-factors for $x = 0$, 0.02, 0.05, 0.1 and 0.15 are 0.00394, 0.00572, 0.00632, 0.00258 and 0.00207. The peaks (without phase correction) near 1.9 and 2.4 Å correspond to the first (Co-Si/Ge) and second (Co-Co) shells of the central Co atom. The fitted data indicate that the coordination number and the bond length do not vary significantly as a function of the dopant Ge concentration. With the increasing dopant concentration ($x = 0$–0.15), the nearest-neighbor Co-Si bond distance is increased from 2.33 Å to 2.36 Å, and the nearest-neighbor Co-Ge bond distance is increased from 2.38 Å to 2.41 Å. The nearest-neighbor Co-Co is approximately 2.71 Å. The EXAFS results imply that the structural symmetry shown in fig. 3(b) remains as a B20 structure upon Ge doping, which is consistent with the

Table 1: Coordination numbers (CN), bond distances (r) and Debye-Waller factors (σ^2) for $CoSi_{1-x}Ge_x$ with $x = 0$–0.15.

x	Shell	CN	r (Å)	σ^2 (10^{-3} Å^2)
0.00	Co-Co	1.96 ± 0.32	2.71 ± 0.01	3.2 ± 0.4
	Co-Si	2.52 ± 0.47	2.33 ± 0.01	5.9 ± 0.8
0.02	Co-Co	1.96 ± 0.32	2.71 ± 0.01	3.6 ± 0.2
	Co-Si	2.39	2.33 ± 0.01	6.0 ± 0.5
	Co-Ge	0.12	2.38 ± 0.01	6.0 ± 0.5
0.05	Co-Co	1.96 ± 0.32	2.71 ± 0.01	3.9 ± 0.3
	Co-Si	2.27	2.34 ± 0.01	6.5 ± 0.5
	Co-Ge	0.25	2.39 ± 0.01	6.5 ± 0.5
0.10	Co-Co	1.96 ± 0.32	2.70 ± 0.01	3.9 ± 0.2
	Co-Si	2.14	2.34 ± 0.01	6.3 ± 0.3
	Co-Ge	0.37	2.39 ± 0.01	6.3 ± 0.3
0.15	Co-Co	1.96 ± 0.32	2.71 ± 0.01	4.4 ± 0.2
	Co-Si	1.76	2.36 ± 0.01	7.2 ± 0.3
	Co-Ge	0.79	2.41 ± 0.01	7.2 ± 0.3

XRD result. The slight expansion of the bond distance upon Ge doping is attributed to the larger atomic radius of Ge than that of Si. The difference in bond distance upon Ge doping may cause local lattice distortion around the central Co atom. DWFs are closely related to the lattice phonon. Therefore, they are further compared in fig. 3(c). The best-fitted DWFs of the Co-Co pair (3.2 ± 0.4 (10^{-3} Å^2)) and Co-Si pair (5.9 ± 0.8 (10^{-3} Å^2)) in the parent compound CoSi are smaller than those of doped ones. The DWFs of Co-Co pair and Co-Si pair, respectively, increase to 4.4 ± 0.2 (10^{-3} Å^2) and 7.2 ± 0.3 (10^{-3} Å^2) in $CoSi_{0.85}Ge_{0.15}$. These results imply that the lattice exhibits more disorder by replacing Si with Ge. Interestingly, the degree of the disorder of Co-Co correlates strongly with lattice thermal conductivity. Figure 3(c) compares the changes in the DWFs and in the lattice thermal conductivity. Ge doping evidently affects lattice disorder, and the point defect can lead to the enhancement of phonon scattering and sequential reduction of lattice thermal conductivity.

The Seebeck coefficient measurement is a sensitive energy probe relative to the Fermi level, and these results could reveal information about the band structure changes. Therefore, XAS results may have a certain extent of correlation with electronic properties above the Fermi (E_F) level. Ge is isoelectronic to Si, so the enhanced thermoelectric performance is probably not due to the changes in the mobility or carrier concentrations; instead, the enhancement is mainly due to the change in the degree of lattice disorder. This study pioneers reporting the use of XAS to comprehensively investigate thermoelectric properties. Improvements in the thermoelectric properties were interpreted on the basis of the variation of local atomic and electronic structures induced by the charge redistribution around the Fermi level and the lattice distortion through chemical substitution. Additionally, this research provides a relevant, rarely used approach to understand thermoelectric materials, as well as lays a foundation in engineering better thermoelectric materials from the perspective of X-ray absorption technique.

Conclusions. – In this study, we exploit XAS to investigate the effects of Ge substitution for Si in cobalt monosilicides on local electronic and atomic structures, as well as their relation to the thermoelectric properties. Spectroscopic observation indicates the occurrence of charge redistribution between Co and Si upon Ge doping. By partially replacing Si with Ge at $x \leq 0.05$, Co gains charges in its $3d$ orbitals. However, this charge is removed from the $3d$ orbitals upon further Ge substitution at $x \geq 0.05$. The thermopower is strongly correlated with the charge redistribution in the Co $3d$ orbital, and the observed charge transfer between Ge and Co is responsible for the variation of Co $3d$ occupancy number. The increase in the lattice phonon by point defect is further evidenced by our spectroscopic results. The disordered Co-Co pair is suggested to dominate the enhancement of phonon scattering. The improvements in the thermoelectric properties, including increased thermopower, suppression of thermal conductivity, and increased figure of merit, are interpreted on the basis of the variation of local atomic and electronic structures studied through X-ray absorption spectroscopy.

* * *

The authors would like to thank the National Science Council of Taiwan for financially supporting this research under contracts NSC 102-2112-M-001-004-MY3 and 101-2112-M-213-004-MY3.

REFERENCES

[1] Pei Y., Shi X., LaLonde A., Wang H., Chen L. and Snyder G. J., *Nature*, **473** (2011) 66.
[2] Fedorov M. I., *J. Thermoelectr.*, **2** (2009) 51.
[3] Schlesinger M. E., *Chem. Rev.*, **90** (1990) 607.
[4] Marklund K., Larsson M., Bystrom S. and Lindqvist T., *Phys. Scr.*, **9** (1974) 47.
[5] Schmitt A. L., Higgins J. M., Szczech J. R. and Jin S., *J. Mater. Chem.*, **20** (2010) 223.
[6] Lue C. S., Kuo Y. K., Huang C. and Lai W., *Phys. Rev. B*, **69** (2004) 125111.
[7] Kim S. W., Mishima Y. and Choi D. C., *Intermetallics*, **10** (2002) 177.
[8] Kuo Y. K., Sivakumar K. M., Huang S. J. and Lue C. S., *J. Appl. Phys.*, **98** (2005) 123510.
[9] Sakai A., Ishii F., Onose Y., Tomioka Y., Yothihashi S., Adachi H., Nagaosa N. and Tokura Y., *J. Phys. Soc. Jpn.*, **76** (2007) 093601.
[10] Ren W. L., Li C. C., Zhang L. T., Ito K. and Wu J. S., *J. Alloys Compd.*, **392** (2005) 50.
[11] Ravel B. and Newville M., *J. Synchrotron Rad.*, **12** (2005) 537.
[12] Heremans J. P., Jovovic V., Toberer E. S., Saramat A., Kurosaki K., Charoenphakdee A.,

Yamanaka S. and Snyder G. J., *Science*, **321** (2008) 554.
[13] Kudryavtsev Y. V., Oksenenko V. A., Lee Y. P., Rhee J. Y. and Kim Y. D., *J. Appl. Phys.*, **102** (2007) 103503.
[14] Pan Z. J., Zhang L. T. and Wu J. S., *Comput. Mater. Sci.*, **39** (2007) 752.
[15] Zhang Z. Z., Partoens B., Chang K. and Peeters F. M., *Phys. Rev. B*, **77** (2008) 155201.
[16] Pan Z. J., Zhang L. T. and Wu J. S., *J. Appl. Phys.*, **101** (2007) 033715.
[17] Ameereh G. I., Hamad B. A. and Khalifeh J. M., *Physica B: Condens. Matter*, **403** (2008) 3503.
[18] Disalvo F. J., *Science*, **285** (1999) 703.